Symmetry Controls the Face Geometry of DNA Polyhedra

7 AUTHORS, INCLUDING:

seung hyeon Ko
Institute for Basic Science
31 PUBLICATIONS   **435** CITATIONS

Wen Jiang
Purdue University
93 PUBLICATIONS   **4,042** CITATIONS

Chengde Mao
Purdue University
135 PUBLICATIONS   **6,492** CITATIONS

# Symmetry Controls the Face Geometry of DNA Polyhedra

Chuan Zhang,[†] Seung Hyeon Ko,[†] Min Su,[‡] Yujun Leng,[†] Alexander E. Ribbe,[†] Wen Jiang,[‡] and Chengde Mao*,[†]

Department of Chemistry, Markey Center for Structural Biology and Department of Biological Sciences, Purdue University, West Lafayette, Indiana 47907

Received December 10, 2008; E-mail: mao@purdue.edu

This Communication reports complementary strategies to control the face geometry during the self-assembly of DNA polyhedra from branched DNA nanomotifs (tiles). In these approaches, the final DNA polyhedra contain two types of DNA tiles. They are different by either sequence or orientation in the final structures. DNA tiles can associate with each other between the two types of different tiles, but not with the same type of tiles. Thus, each face must contain an even number of tiles. As a demonstration, DNA cubes, whose faces are squares that contain four tiles, have been assembled through these approaches. The cube structures have been confirmed by multiple techniques including polyacrylamide gel electrophoresis (PAGE), dynamic light scattering (DLS), cryogenic electron microscopy (cryo-EM) imaging, and single particle three-dimensional (3D) reconstruction.

DNA has been shown as a superb molecular system in self-assembly toward bottom-up nanofabrication.[1] In the last two decades, a range of DNA motifs have been developed, and complicated 1D,[2] 2D,[3] and 3D[4] large nanostructures have been fabricated. Recently, we have shown that one-component star-shaped DNA motifs can assemble into a range of geometrically well-defined polyhehedra including tetrahedra, dodecahedra, and buckyballs from 3-point-star motifs,[5] and icosahedra and large nanocages from 5-point-star motifs.[6] It is achieved by carefully balancing the flexibilities and the rigidities of the motifs and controlling the DNA concentrations. Each vertex consists of a star tile and the separation between any two adjacent vertices is integral numbers of turns. With such a separation, all tiles face to the same side and the tiles' intrinsic curvatures accumulate at the same direction, which promotes the formation of closed structures instead of extended sheets. One face of the polyhedra can contain any number of vertices. It is straightforward to expand the list of the structures we can achieve by using different building blocks, for example, assembling octahedral structures from four-point-star motifs. However, to further expand the structural scope, novel assembly strategies, in addition to controlling the flexibility and the concentration of DNA tiles, are needed. Herein, we report such strategies to restrict polyhedral faces to consist of only even numbers of vertices and use such strategies to assemble DNA cubes, the symbol for DNA nanotechnology.[4a]

A cube consists of eight vertices and each vertex can be represented by a three-point-star tile. Each face is a square and consists of four three-point-star tiles. This requirement cannot be met by simply changing the concentration and the flexibility of the DNA tiles. To overcome this problem, we exploit the helical nature of the DNA double helix structure. When being separated by odd numbers of half-turns, two objects along a DNA duplex will be on the opposite sides of the DNA duplex and are related by a 2-fold
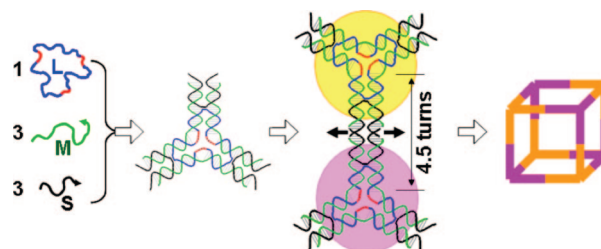
Figure 1. Self-assembly of DNA 4.5-turn cubes from eight copies of identical three-point-star tiles. Individual DNA single strands recognize and associate with each other to form three-point-star tiles, and then assemble into DNA cubes. The separation of any two adjacent tiles is 4.5 DNA helical turns; thus, the resulting DNA cubes are named 4.5-turn cubes. Note that any two interacting tiles (shadowed golden and purple) are related by a 2-fold rotational axis, indicated by arrowed black lines.

rotational symmetry. When any two three-point-star tiles are associated through hybridization of sticky ends, they are designed to be separated by 4.5 DNA helical turns (Figure 1). The odd number of helical half-turns leads the adjacent tiles to face to different sides of the DNA plane. To assemble into closed rings, each ring has to contain an even number of tiles. The smallest polyhedron that meets this requirement is a cube; which suggests that the three-point-star motif at sufficiently low concentrations will assemble into cubes (Figure 1). The three-point-star motif consists of a long, three-repeating, central DNA strand (**L**, blue-red), three medium strands (**M**, green), and three short strands (**S**, black). To ensure DNA tiles to have sufficient flexibility to bend in either direction (up or down from the plane), three 5-base-long, single-stranded loops (red) are introduced into the central DNA strand **L** (the red segments). Such a design promotes all tiles to bend inward to form closed 3D structures (cubes).

DNA self-assembly is a one-pot process. When individual DNA single strands are mixed and slowly cooled from 95 to 22 °C, they stepwise assemble into individual three-point-star tiles and, then cubes. A cube contains two sets of DNA tiles (golden and purple). They are identical when being free, individual tiles, but bend in opposite directions relative to their own structures when being incorporated into the cubes. After assembly, the DNA sample is first analyzed by native PAGE (Figure 2a). At a low DNA concentration (50 nM) and a correct molecular ratio (L:M:S = 1:3:3), most of the DNAs are incorporated into a large, well-defined, molecular complex, which corresponds to the sharp band appearing in the gel. The assembly yield is ∼ 82% as estimated from the gel by an image processing software, ImageJ (developed at the National Institute of Health, NIH). DLS studies reveal that the DNA complex has an apparent hydrodynamic radius of 16.0 ± 2.8 nm (Figure 2b). This value agrees well with the radius of the circumscribed sphere of the DNA cube (16.5 nm), assuming the standard B-DNA conformation (pitch, 0.33 nm/base pair; diameter, 2 nm).
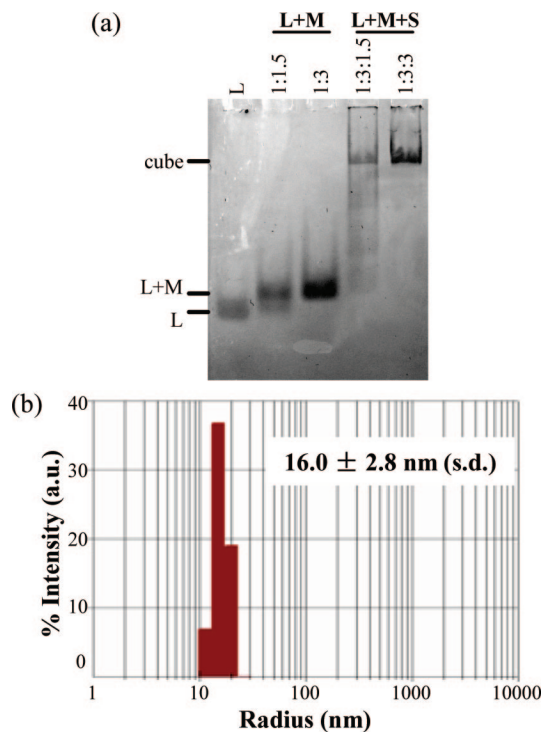
Figure 2. Characterization of the 4.5-turn DNA cubes. (a) Native polyacrylamide gel electrophoretic (PAGE) analysis. The sample in each lane and the identities of the main bands were indicated above and at the left of the gel image, respectively. (b) Size histogram of the 4.5-turn cubes measured by dynamic light scattering (DLS).

To provide direct structural characterization, we imaged the DNA samples with cryoEM by following previously reported procedures (Figure 3).[5,6] A thin layer of sample solution is flash frozen. Under such conditions, the DNA complexes are likely kept in their native conformations. Most particles observed in cryo-EM images are consistent with the 2D projections of cubes at the expected size (Figure 3a and Supporting Information, Figure S1). With experimentally observed particles, a DNA cube structure (Figure 3c) at ~2.9 nm resolution is revealed by a technique of 3D single particle reconstruction,[7] a proven technique routinely used in structural virology. The cube edge is ~15 nm long, nicely matching the value calculated from the design (15.5 nm). By comparing the 2D projections of the reconstructed cube model and the raw images with similar orientations (Figure 3b), clear similarities confirm that the self-assembled DNA complex indeed has a cube structure. A further support for the reconstructed model comes from the comparison between the computed projections from model and the class averages of raw particle images with similar views (Supporting Information, Figure S2).

The above-discussed approach allows self-assembly of cubes from one component three-point-star motif. This strategy is not an obvious derivative of the previously used strategy for self-assembly of tetrahedra[5] and icosahedra.[6] A straightforward derivative strategy is to use two different component three-point-star motifs A and B (Figure 4). They have the same backbone structures but different DNA sequences. Their sticky-ends are complementary to each other, but not self-complementary. Thus, they can only associate between different motifs but not among the same motifs. This design ensures that a closed complex must contain an equal number of tiles A and B; and the number of total tiles is even. A smallest such polyhedron would be a cube as for the above-discussed strategy. Tiles A and B are formed separately and then mixed at 40 °C at a low DNA concentration (200 nM of each tile). When further cooling down
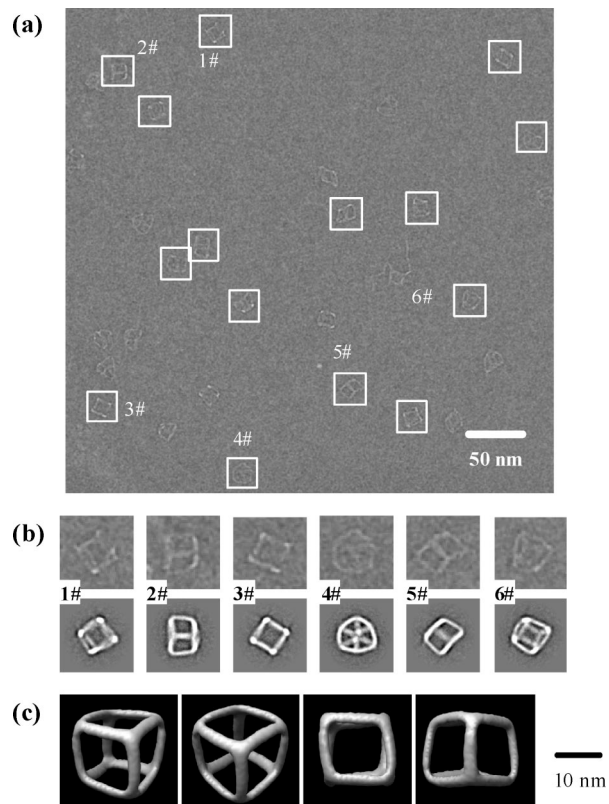

Figure 3. Cryo-EM images and reconstructions of the 4.5-turn DNA cubes: (a) a raw cryo-EM image of the DNA sample; (b) close-up view of several representative raw particles from panel a (upper row) and their corresponding computer-generated model projections (lower row); (c) the 3D reconstruction maps of the DNA cube, reconstructed by imposing a tetrahedron symmetry.
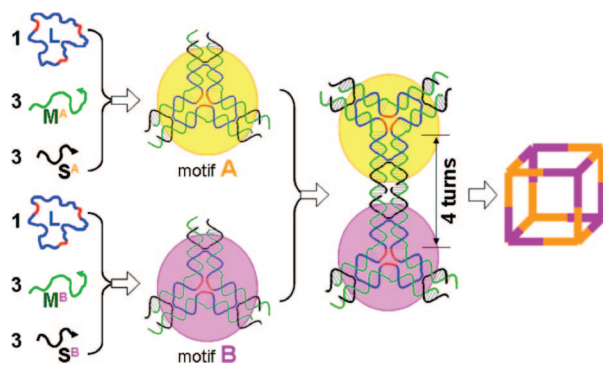
Figure 4. Assembly of DNA 4-turn cubes from two different component three-point-star tiles (A and B). Tiles A and B can associate with each other but can not associate with themselves, resulting in that each face must consist of even number of tiles. The separation of any two adjacent tiles is 4 DNA helical turns; thus, the resulting DNA cubes are named 4-turn cubes. The separation of an integral number of turns ensures that all tiles face to the same side of the DNA plane and promotes DNA complex cyclization.

from 40 °C to room temperature occurs, the tiles A and B associate together into cubes. Again, the DNA complexes are checked by native PAGE and DLS (Figure 5). Different from the single-tile design (4.5-turn cubes), four DNA helical turns are used for the edge length of the cube to promote complex cyclization. Such 4-turn cubes have slightly smaller sizes than the 4.5 turn cubes. In PAGE gel, a main band appears when mixing those two 3-point-star motifs. It moves much slower than the individual motifs but slightly faster than the 4.5-turn cubes owing to the size difference (Figure 5a).
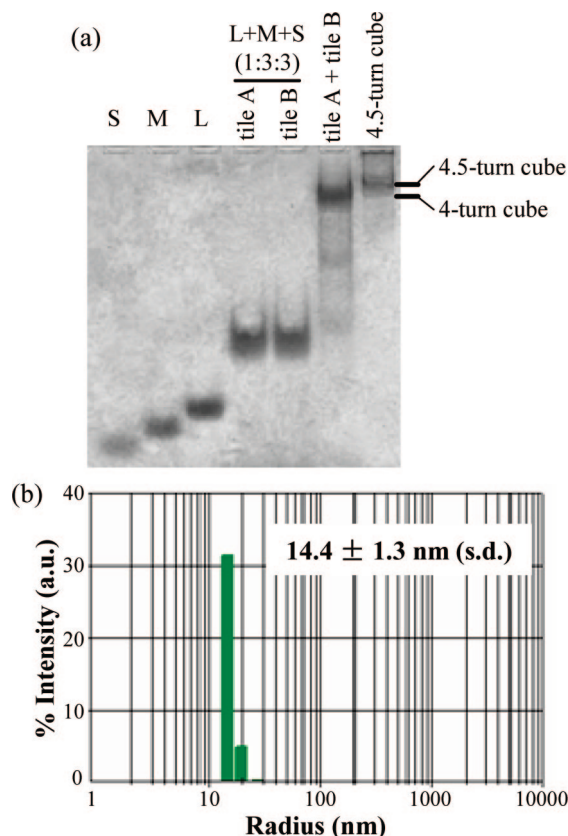
Figure 5. Characterization of the 4-turn DNA cubes. (a) Native PAGE analysis of 4-turn DNA cubes. Equal molar mixing of tiles A and B resulted in the self-assembly of 4-turn cubes, which appear as a sharp band with a slightly faster migration rate than that of the slightly larger 4.5-turn DNA cubes. (b) Size histogram of the 4-turn cubes measured by DLS.

DLS study shows the radius of the DNA complex is 14.4 nm (Figure 5b), nicely matching with the design of the 4-turn cube (15.0 nm).

The key criterion of these strategies is that each face contains an even number of vertices. A large number of polyhedra, for example, cubes, hexagonal and octagonal prisms, and truncated octahedra, all fit this criterion. Cubes are the smallest member of this family. Because low concentration favors small assemblies, sufficiently low DNA concentrations (as in our current study) will kinetically control the self-assembly process to selectively generate cubes, the smallest structure.

In summary, two complementary strategies have been exploited to control the face geometry in self-assembly of discrete DNA 3D structures. They allow assembling DNA cubes from either eight identical three-point-star tiles or two types of different tiles (four for each). In addition to two previously reported strategies (controlling flexibility and concentration of DNA tiles) for structural controls over DNA 3D self-assembly,[5,6] this work has introduced a new element: taking advantage of the helical nature of DNA duplexes to orient the DNA tiles. We believe that the interplay of these three strategies will likely expand the scope of the DNA 3D

discrete structures that we can assemble. Experimental explorations along this direction are conducted in our research group.

Supporting Information Available: Complete ref 4h; experimental method and additional experimental data. This material is available free of charge via the Internet at http://pubs.acs.org.

References

(1) For recent reviews on DNA self-assembly, see: (a) Seeman, N. C. *Nature* **2003**, *421*, 427–431. (b) Lin, C.; Liu, Y.; Rinker, S.; Yan, H. *ChemPhysChem* **2006**, *7*, 1641–1647. (c) Aldaye, F. A.; Palmer, A. L.; Sleiman, H. F. *Science* **2008**, *321*, 1795–1799.

(2) (a) Mitchell, J. C.; Malo, J. R.; Bath, J.; Turberfield, A. J. *J. Am. Chem. Soc.* **2004**, *126*, 16342–16343. (b) Rothemund, P. W. K.; Ekani-Nkodo, A.; Papadakis, N.; Kumar, A.; Fygenson, D. K.; Winfree, E. *J. Am. Chem. Soc.* **2004**, *126*, 16344–16352. (c) Liu, D.; Park, S. H.; Reif, J. H.; LaBean, T. H. *Proc. Natl. Acad. Sci. U.S.A.* **2004**, *101*, 717–722. (d) Liu, H.; Chen, Y.; He, Y.; Ribbe, A. E.; Mao, C. *Angew. Chem., Int. Ed.* **2006**, *45*, 1942–1945. (e) Yin, P.; Hariadi, R. F.; Sahu, S.; Choi, H. M. T.; Park, S. H.; LaBean, T. H.; Reif, J. H. *Science* **2008**, *321*, 824–826. (f) Park, S. H.; Barish, R.; Li, H.; Reif, J. H.; Finkelstein, G.; Yan, H.; LaBean, T. H. *Nano Lett.* **2005**, *5*, 693–696. (g) Ghodke, H. B.; Krishnan, R.; Vignesh, K.; Kumar, G. V. P.; Narayana, C.; Krishnan, Y. *Angew. Chem., Int. Ed.* **2007**, *46*, 2646–2649. (h) Weizmann, Y.; Braunschweig, A. B.; Wilner, O. I.; Cheglakov, Z.; Willner, I. *Proc. Natl. Acad. Sci. U.S.A.* **2008**, *105*, 5289–5294. (i) Yin, P.; Choi, H. M. T.; Calvert, C. R.; Pierce, N. A. *Nature* **2008**, *451*, 318–322.

(3) (a) Winfree, E.; Liu, F.; Wenzler, L. A.; Seeman, N. C. *Nature* **1998**, *394*, 539–544. (b) LaBean, T. H.; Yan, H.; Kopatsch, J.; Liu, F.; Winfree, E.; Reif, J. H.; Seeman, N. C. *J. Am. Chem. Soc.* **2000**, *122*, 1848–1860. (c) Mao, C.; Sun, W.; Seeman, N. C. *J. Am. Chem. Soc.* **1999**, *121*, 5437–5443. (d) Yan, H.; Park, S. H.; Finkelstein, G.; Reif, J. H.; LaBean, T. H. *Science* **2003**, *301*, 1882–1884. (e) Liu, D.; Wang, M.; Deng, Z.; Walulu, R.; Mao, C. *J. Am. Chem. Soc.* **2004**, *126*, 2324–2325. (f) Ding, B.; Sha, R.; Seeman, N. C. *J. Am. Chem. Soc.* **2004**, *126*, 10230–10231. (g) Rothemund, P. W. K.; Papadakis, N.; Winfree, E. *PLoS Biology* **2004**, *2*, 2041–2053. (h) Malo, J.; Mitchell, J. C.; Venien-Bryan, C.; Harris, J. R.; Wille, H.; Sherratt, D. J.; Turberfield, A. J. *Angew. Chem., Int. Ed.* **2005**, *44*, 3057–3061. (i) Mathieu, F.; Liao, S.; Kopatsch, J.; Wang, T.; Mao, C.; Seeman, N. C. *Nano Lett.* **2005**, *4*, 661–665. (j) Severcan, I.; Koyfman, A. Y.; Weinkam, P.; Oroudjev, E.; Hansma, H. G.; Jaeger, L. *Science* **2004**, *306*, 2068–2072. (k) Chelyapov, N.; Brun, Y.; Gopalkrishnan, M.; Reishus, D.; Shaw, B.; Adleman, L. *J. Am. Chem. Soc.* **2004**, *126*, 13924–13925. (l) He, Y.; Tian, Y.; Ribbe, A. E.; Mao, C. *J. Am. Chem. Soc.* **2006**, *128*, 15978–15979. Rothemund, P. W. K. *Nature* 2006, *440*, 297−302. (m) Jungmann, R.; Liedl, T.; Sobey, T. L.; Shih, W.; Simmel, F. C. *J. Am. Chem. Soc.* **2008**, *130*, 10062–10063. (n) Park, S. H.; Finkelstein, G.; LaBean, T. H. *J. Am. Chem. Soc.* **2008**, *130*, 40–41.

(4) (a) Chen, J. H.; Seeman, N. C. *Nature* **1991**, *350*, 631–633. (b) Zhang, Y. W.; Seeman, N. C. *J. Am. Chem. Soc.* **1994**, *116*, 1661–1669. (c) Shih, W. M.; Quispe, J. D.; Joyce, G. F. *Nature* **2004**, *427*, 618–621. (d) Goodman, R. P.; Schaap, I. A. T.; Tardin, C. F.; Erben, C. M.; Berry, R. M.; Schmidt, C. F.; Turberfield, A. J. *Science* **2005**, *310*, 1661–1665. (e) Aldaye, F. A.; Sleiman, H. F. *J. Am. Chem. Soc.* **2007**, *129*, 13376–13377. (f) Jonoska, N.; Twarock, R. *J. Phys. A* **2008**, 304043. (g) Zimmermann, J.; Cebulla, M. P. J.; Monninghoff, S.; von Kiedrowski, G. *Angew. Chem., Int. Ed.* **2008**, *47*, 3626–3630. (h) Andersen, F. F.; et al. *Nucleic Acid Res.* **2008**, *36*, 1113–1119.

(5) He, Y.; Ye, T.; Su, M.; Zhang, C.; Ribbe, A. E.; Jiang, W.; Mao, C. *Nature* **2008**, *452*, 198–201.

(6) Zhang, C.; Su, M.; He, Y.; Zhao, X.; Fang, P.; Ribbe, A. E.; Jiang, W.; Mao, A. *Proc. Natl. Acad. Sci. U.S.A.* **2008**, *105*, 10665–10669.

(7) Ludtke, S. J.; Baldwin, P. R.; Chiu, W. *J. Struct. Biol.* **1999**, *128*, 82–97.

JA809666H